

Ablation of the Ccr2 gene exacerbates polyarthritis in interleukin-1 receptor antagonist-deficient mice

メタデータ	言語: eng 出版者: 公開日: 2017-10-05 キーワード (Ja): キーワード (En): 作成者: メールアドレス: 所属:
URL	https://doi.org/10.24517/00027537

This work is licensed under a Creative Commons Attribution-NonCommercial-ShareAlike 3.0 International License.



Ablation of CC chemokine receptor 2 gene exacerbates the polyarthritis in interleukin-1 receptor antagonist-deficient mice

Hiroshi Fujii,¹ Tomohisa Baba,² Yuko Ishida,³ Toshikazu Kondo,³ Masakazu Yamagishi,¹ Mitsuhiro Kawano,¹ and Naofumi Mukaida²

¹Hiroshi Fujii, MD, Masakazu Yamagishi, MD, PhD, Mitsuhiro Kawano, MD, PhD: Division of Rheumatology, Department of Internal Medicine, Graduate School of Medical Science, and ²Tomohisa Baba, PhD, Naofumi Mukaida, MD, PhD: Division of Molecular Bioregulation, Cancer Research Institute, Kanazawa University, Kanazawa 920-1192, Japan, and ³Yuko Ishida, PhD, Toshikazu Kondo, MD, PhD: Department of Forensic Medicine, Wakayama Medical University, Wakayama 641-8509, Japan

Addressed correspondence and reprint requests to Naofumi Mukaida, MD, PhD, Division of Molecular Bioregulation, Cancer Research Institute, Kanazawa University, Kanazawa 920-1192, Japan. Telephone number, +81-76-264-6735; Fax, +81-76-234-4520; E-mail, naofumim@kenroku.kanazawa-u.ac.jp

Subtitle: Exacerbation of arthritis by CCR2 gene ablation

Conflict of interest: The authors have declared that no conflict of interest exists.

Abstract

Objective. The pathogenesis of rheumatoid arthritis (RA) involves cytokines and chemokines. Intraarticular macrophage infiltration in RA prompted us to address the pathogenic role of CC chemokine receptor 2 (CCR2), a chemokine receptor, which is abundantly expressed by macrophages, in an RA model, the arthritis in IL-1 receptor antagonist (*Il1rn*)-deficient mice.

Methods. *Il1rn*-deficient and *Il1rn-CCR2*-doubly deficient mice underwent clinical assessment of arthritis and histological examination. Bone mineral density was measured with computed tomography. The types of cells infiltrating joints were determined by immunohistochemical analysis and flow cytometric analysis. Osteoclasts in joints were quantified after tartrate-resistant acid phosphatase (TRAP) staining. Cytokine and chemokine levels were measured by enzyme-linked immunosorbent assay and multiplex suspension array assay. The expression patterns of chemokines and osteoclastogenic factors were determined by double-color immunofluorescence analysis. Anti-mouse CXC chemokine receptor (CXCR) 2 antibody was injected to *Il1rn-Ccr2*-doubly deficient mice for blocking experiments.

Results. Ablation of *Ccr2* gene actually exaggerated arthritis and intraarticular osteoclastogenesis, while it enhanced intraarticular neutrophil but not macrophage accumulation in *IL-1rn*-deficient mice. Infiltrated neutrophils expressed osteoclastogenic factors, receptor of activator of NF- κ B ligand (RANKL) and a disintegrin and metalloproteinase (ADAM) 8, thereby augmenting intraarticular osteoclastogenesis in *Il1rn-Ccr2*-doubly deficient mice. Moreover, the double-deficient mice exhibited enhanced expression of neutrophilic chemokines, keratinocyte chemoattractant (KC) and macrophage inflammatory protein 2 (MIP-2), compared with *IL-1rn*-deficient mice. Finally, neutralizing antibodies to CXCR2, the receptor for KC and MIP-2, dramatically attenuated arthritis in *Il1rn-Ccr2*-doubly deficient mice.

Conclusion. CCR2-mediated signals can modulate the arthritis in *Il1rn*-deficient mice by negatively regulating neutrophil infiltration.

Introduction

Rheumatoid arthritis (RA), a chronic inflammatory disorder of synovium, cartilage, and bone, affects about 1 % of the population and is associated with a substantial morbidity and an increased mortality (1). In RA, various inflammatory cells such as macrophages, neutrophils, and lymphocytes, infiltrate into the synovium and periarticular space. Among inflammatory cells, macrophages have a major pathogenic role in RA, because macrophages are a major cellular source of tumor necrosis factor (TNF)- α , interleukin (IL)-1 α , and IL-1 β , the cytokines that are presumed to be crucially involved in the pathogenesis and/or progression of RA (1, 2). Indeed, the macrophage numbers in synovium correlates well with clinical symptoms and joint damages in RA (3). Moreover, various therapeutic modalities attenuated RA symptoms along with a reduction in synovial macrophage numbers (4). Thus, inhibition of intrasynovial macrophage accumulation can prevent disease progression in RA.

Chemokines represent a large superfamily of small proteins, which can regulate trafficking and activation of various types of cells, particularly leukocytes under both inflammatory and homeostatic conditions. Chemokines can exert their actions by binding their cognate G protein-coupled receptors expressed on the target cells. Thus, the types of expressed chemokine receptors can determine the responsiveness of leukocytes to particular chemokines (5). Macrophages express a number of chemokine receptors, particularly abundantly CCR2, a selective receptor for a major macrophage-tropic chemokine, Chemokine (C-C motif) ligand 2 (CCL2)/monocyte chemoattractant protein (MCP)-1. Mirroring abundant macrophage infiltration into joint cavities, CCL2 levels were markedly increased in RA joints (6), and inhibition of either CCL2 or CCR2 can ameliorate symptoms and signs observed in various rodent models of arthritis (7, 8). Moreover, recent studies have demonstrated that CCL2 can promote osteoclastogenesis in vitro (9, 10). These observations raised the possibility that CCR2 could be a target to regulate arthritis. However, clinical intervention by anti-CCR2 or anti-CCL2 antibody failed to induce the expected improvement when given to RA patients (11, 12). Similarly, CCR2 antagonist

failed to improve anti-collagen antibody-induced arthritis (13). Furthermore, Quinones and colleagues demonstrated that *Ccr2* gene ablation even aggravated collagen-induced arthritis (14). These discrepancies may be explained by an observed dual role of CCR2 during initiation and progression of collagen-induced arthritis (15), but require further investigation.

Although IL-1 α and IL-1 β are transcribed from two distinct genes, both have similar biological activities after binding to a common IL-1 receptor and can behave as essential mediators of tissue destruction in various inflammatory disorders such as sepsis and RA (16, 17). IL-1 receptor antagonist (IL-1ra; gene name, *IL-1rn*) is a member of the IL-1 family and exhibits an identical β -pleated sheet structure as IL-1s. IL-1ra can bind to IL-1 receptor at the same sites with a similar affinity as IL-1s (18), but cannot associate with IL-1 receptor accessory protein, which is indispensable for the biological activities of IL-1s (19, 20). Thus, IL-1ra is a natural competitive antagonist of IL-1s and can negatively regulate the bioactivities of IL-1s in various inflammatory conditions. Actually, the combination therapy of methotrexate with recombinant human IL-1ra protein, provided significantly greater clinical benefits to patients with RA than methotrexate alone (21). Moreover, the analysis on human *IL-1rn* gene polymorphism revealed that homozygosity for *IL-1RN*2* was associated with lower plasma IL-1ra levels (22) and with an increased number of affected articular areas in RA patients (23). Furthermore, polyarthritis spontaneously develops in *IL-1rn*-deficient BALB/c mice and resembles human RA (24). Thus, *IL-1rn*-deficient BALB/c mice can be a good animal model for RA.

Gene expression profiles revealed that the joints of *Il1rn*^{-/-} mice exhibited enhanced mRNA expression of chemokines including CCL2/MCP-1, CCL8/MCP-2, CCL7/MCP-3, CCL5, Chemokine (C-X-C motif) ligand (CXCL) 1, and CXCL12 (25). Moreover, further analysis demonstrated enhanced expression of the genes encoding receptors for these chemokines, such as CCR2, CCR5, CXCR2, and CXCR4 (25). In order to delineate the pathogenic roles of CCR2-mediated signals in polyarthritis, we generated mice lacking both *Il1rn* and *Ccr2* genes, by mating *Il1rn*^{-/-} with *Ccr2*^{-/-} mice. Intriguingly,

osteoclastogenesis and polyarthritis were enhanced in these doubly deficient mice, compared with *Il1rn*^{-/-} mice. Thus, CCR2-mediated signals could dampen pathological osteoclastogenesis in arthritic joints.

Materials and Methods

Mice

BALB/c mice were purchased from Charles River Japan (Yokohama, Japan) and were designated as wild-type (WT) mice. *Il1rn*^{-/-} mice were generated as previously described (26). *Ccr2*^{-/-} mice were kind gifts from Dr. William Kuziel (University of Texas San Antonio, San Antonio, TX) (27). *Ccr2*^{-/-} mice were backcrossed to BALB/c mice for eight to ten generations. *Il1rn*^{-/-}*Ccr2*^{-/-} mice were generated by crossing *Il1rn*^{-/-} mice with *Ccr2*^{-/-} mice. All animal experiments were performed under specific pathogen-free conditions in accordance with the Guideline for the Care and Use of Laboratory Animals of Kanazawa University.

Assessment of arthritic sign and histology

Each limb was examined weekly on a scale of 0 to 3 as previously reported (28). Ankle joints were obtained from 8-, 12-, 16- and 20-week-old mice. Joints were fixed in 4 % paraformaldehyde, decalcified in 10% EDTA-4Na, and embedded in paraffin. Sections were stained with hematoxylin and eosin. Histopathological changes were scored as previously described (28) by an examiner without any previous knowledge on the genetic background of the mice. Joint sections were stained for TRAP with Leukocyte Acid Phosphatase kit (Sigma-Aldrich, St. Louis, MO, USA), according to the manufacturer's instructions. Slides were subjected to counterstaining with methyl green. Osteoclasts were identified as TRAP-positive cells with at least 2 nuclei, and were determined separately in synovial tissue and subchondral bone marrow. Some paraffin-embedded sections were stained with rat anti-mouse F4/80, anti-mouse CD3 (Serotec, Kidlington, UK), or anti-mouse Ly-6G antibodies (BD Biosciences, San Jose, CA, USA). The sections were then incubated with biotinylated rabbit anti-rat IgG (Dako, Glostrup, Denmark). The immune complexes were visualized using a catalyzed signal amplification system (Dako) or the ELITE avidin-biotin-peroxidase and diaminobenzidine substrate kits (Vector Laboratories, Burlingame, CA, USA). When rat IgG (Cosmo Bio, Tokyo, Japan) was used

instead of specific primary antibodies as a negative control, no staining was observed (data not shown), indicating the specificity of the reactions. Positive cell numbers were determined in 5 randomly chosen fields at 400-fold magnification in each synovial tissue.

Flow cytometric analysis

Bone marrow cells were obtained from femoral and tibial bones of 8- or 20-week old mice. Joints were obtained from 10- or 20-week old animals and were digested with collagenase type I (Wako, Osaka, Japan). The single cell suspensions from bone marrow or joints were stained with various combinations of fluorescein isothiocyanate (FITC)-conjugated anti-CD3, phycoerythrin (PE)-conjugated anti-CD4, allophycocyanin (APC)-conjugated anti-CD8, PE-conjugated anti-B220, APC-conjugated CD11c, FITC-conjugated anti-Ly-6C (Abcam, Cambridge, MA, USA), PE-conjugated anti-Ly-6G, APC-conjugated anti-CD11b monoclonal antibodies (eBioscience, San Diego, CA, USA) . Cell surface marker expression was analyzed using a FACSCalibur (BD Biosciences) with Cell Quest analysis software (BD Biosciences).

Double-color immunofluorescence analysis

Paraffin-embedded joint sections from 20-week-old *Il1rn^{-/-}Ccr2^{-/-}* mice were stained with various combinations using goat anti-RANKL (R&D Systems, Minneapolis, MN), rabbit anti-KC (BioVision, Mountain View, CA, USA), goat anti-MIP2 (R&D System), rat anti-Ly-6G, rat anti-CD3 and rat anti-F4/80 antibodies. Cells infiltrating the joints were isolated as described above and were centrifuged to prepare cytospin sections. After fixation in methanol, sections were incubated with goat anti-ADAM 8 (Santa Cruz Biotechnology, Santa Cruz, CA, USA), together with anti-Ly-6G, anti-CD3, or anti-F4/80 antibodies. After washing, the sections were incubated with Alexa Fluor 488-labeled donkey anti-rat IgG antibodies and Alexa Fluor 546-labeled donkey anti-goat IgG or Alexa Fluor 594-labeled donkey anti-rabbit IgG antibodies (Molecular Probes, Carlsbad, CA, USA). Immunofluorescence was visualized in a dual channel mode on a fluorescence

microscope.

Assessment of bone mineral density

Total bone mineral densities of the four limbs were determined on 20-week old mice by using Latheta computed tomography system (Aloka, Tokyo, Japan), according to the manufacturer's instructions.

Determination of cytokine and protein levels

Cartilage oligomeric matrix protein (COMP) assay kit (Anamar, Goteborg, Sweden) and TRAP5b assay kit (Immunodiagnostic Systems, Inc, Boldon, UK) were used to determine serum COMP and TRAP5b levels, respectively. Joint tissues were obtained from animals at the indicated time points and homogenized with RIPA buffer (Santa Cruz Biotechnology) containing proteinase inhibitor cocktail and centrifuged to obtain supernatants. After determining total protein contents with a BCA kit (Pierce, Rockford, IL), macrophage (M)-colony stimulating factor (CSF), RANKL (R&D Systems), and ADAM 8 (Cusabio Biotech, Wuhan, Hubei, China) levels were determined using specific ELISA kits for these molecules, according to the manufacturer's instructions. IL-17A, granulocyte (G)-CSF, KC, and MIP-2 levels were determined by using a multiplex suspension array system (Bio-rad Laboratories Inc., Hercules, CA, USA) according to the manufacturer's instructions. The data are expressed as the target molecule (pg) per total protein (mg) for each sample.

Treatment with neutralizing Ab against mouse CXCR2

Anti-mouse CXCR2 rabbit IgG were prepared as previously reported (29) and used for blocking experiments. *Il1rn^{-/-}Ccr2^{-/-}* mice were injected intraperitoneally with 200 µg of anti-mouse CXCR2 rabbit IgG or normal rabbit IgG, both twice a week from 12 weeks of age until 16 weeks of age. Mice were sacrificed 24 hours after the last injection and joint pathology and the number of infiltrating neutrophils were analyzed as described above.

Statistical analysis

Data were analyzed statistically using one-way ANOVA followed by the Fisher protected least significant difference test. Mann-Whitney's U test or Kuraskal Wallis test was used in instances when the data was not normally distributed. $p < 0.05$ was considered statistically significant.

Results

***Ccr2* deletion aggravated spontaneously developed polyarthritis developed in *Il1rn*^{-/-} mouse**

Consistent with the previous observation (24), *Il1rn*-deficient mice spontaneously developed polyarthritis until 12 weeks after birth. *Ccr2*^{-/-} mice did not exhibit any signs indicative of arthritis until 1 year after birth (data not shown). Body weight gain was retarded in *Il1rn*^{-/-}*Ccr2*^{-/-} after 14 weeks of age compared to *Il1rn*^{-/-} mice (Figure 1A). The incidence and the onset time of disease were comparable between these two strains (data not shown). However, after 16 weeks of age, *Il1rn*^{-/-}*Ccr2*^{-/-} mice exhibited higher arthritis score with extensive swelling and severe ankylosing in multiple joints, than *Il1rn*^{-/-} mice with mild joint inflammation restricted to hind paws (Figure 1A). WT and *Ccr2*^{-/-} mice showed no histological signs of arthritis until 1 year after birth (data not shown). Histological signs of synovial inflammation appeared in *Il1rn*^{-/-} and *Il1rn*^{-/-}*Ccr2*^{-/-} mice at 8 weeks after birth, with no apparent differences until 12 weeks. Signs of joint inflammation such as cartilage damage, bone erosion, and cell infiltration, were augmented in *Il1rn*^{-/-}*Ccr2*^{-/-} mice at 16 week after birth and later, compared with *Il1rn*^{-/-} mice (Figure 1B). Computed tomographical analysis consistently demonstrated greater decrease in bone mineral density in *Il1rn*^{-/-}*Ccr2*^{-/-} mice than *Il1rn*^{-/-} mice (Figure 1C). Moreover, serum concentration of COMP, a marker of cartilage destruction, was increased to a greater extent in *Il1rn*^{-/-}*Ccr2*^{-/-} mice than *Il1rn*^{-/-} mice (Figure 1D). These observations indicate that the lack of a *Ccr2* gene exacerbated the polyarthritis in *Il1rn*^{-/-} mice, together with enhanced intraarticular inflammation and bone destruction.

***Ccr2* deficiency enhanced neutrophil infiltration in *Il1rn*^{-/-} mouse**

The enhanced intraarticular cell infiltration in *Il1rn*^{-/-}*Ccr2*^{-/-} mice prompted us to investigate the types of cells infiltrating joints. Immunohistochemical analyses demonstrated that a

small number of CD3-positive T cells and F4/80-positive monocytes infiltrated the joints in *Il1rn^{-/-}* and *Il1rn^{-/-}Ccr2^{-/-}* mice at 8 week after birth and that their numbers increased marginally and to similar extents in *Il1rn^{-/-}* and *Il1rn^{-/-}Ccr2^{-/-}* mice, thereafter (Figure 2A and Supplementary Figure 1). On the contrary, Ly6G-positive neutrophils markedly infiltrated the joints in *Il1rn^{-/-}* and *Il1rn^{-/-}Ccr2^{-/-}* mice beginning at 12 week after birth, and the increase was more evident in *Il1rn^{-/-}Ccr2^{-/-}* mice than *Il1rn^{-/-}* mice (Figure 2A and Supplementary Figure 1). Flow cytometric analyses of infiltrating cells in the joints consistently revealed an augmented increase in the relative and absolute numbers of Ly-6G-positive neutrophils, but not F4/80-positive macrophages, CD4-positive T lymphocytes, CD8-positive T lymphocytes, B220-positive B lymphocytes, or CD11c-positive dendritic cells in *Il1rn^{-/-}Ccr2^{-/-}* mice, compared with *Il1rn^{-/-}* mice (Figure 2B, C). These observations would indicate that the absence of *Ccr2* gene selectively augmented intraarticular neutrophil infiltration.

***Ccr2* deficiency increased osteoclast numbers in *Il1rn^{-/-}* mouse.**

Enhanced bone destruction in *Il1rn^{-/-}Ccr2^{-/-}* mice prompted us to determine the numbers of osteoclasts, the cell which is mainly responsible for bone resorption. TRAP staining demonstrated that osteoclast numbers in joints were increased progressively in *Il1rn^{-/-}* and *Il1rn^{-/-}Ccr2^{-/-}* mice and that the increase was more evident in *Il1rn^{-/-}Ccr2^{-/-}* mice than in *Il1rn^{-/-}* mice (Figure 3A and Supplementary Figure 2A). Moreover, serum concentration of TRAP5b, an indicator of osteoclast activity, was increased in *Il1rn^{-/-}Ccr2^{-/-}* mice to a greater extent than *Il1rn^{-/-}* mice (Figure 3B). Clinical studies on RA patients imply bone edema as an important parameter to predict prognosis (30). Because bone edema is pathologically characterized by osteoclast infiltration into subchondral bone marrow (31), we determined TRAP-positive cell numbers in subchondral bone marrow. Indeed, TRAP-positive cell numbers were increased in the subchondral bone marrow in *Il1rn^{-/-}Ccr2^{-/-}* mice to larger extents than in *Il1rn^{-/-}* mice (Figure 4A and Supplementary Figure 2B). Several lines of evidence indicate the essential roles of *Ccr2*-mediated signals in the egress of macrophages,

a precursor of osteoclasts from bone marrow. Ly-6G^{low}Ly-6C-positive macrophage numbers in bone marrow were consistently increased in *Il1rn*^{-/-}*Ccr2*^{-/-} mice compared with *Il1rn*^{-/-} mice (Figure 4B and Supplementary Figure 3). These observations would indicate that *Ccr2* deficiency increased the numbers of intra-bone marrow macrophages, a precursor of osteoclasts, and simultaneously increased the number of osteoclasts in synovium and bone marrow.

Increased expression of osteoclastogenic factors by neutrophils

The enhanced osteoclastogenesis impelled us to determine the intraarticular levels of major osteoclastogenic factors, such as M-CSF, RANKL, and ADAM 8. There were no significant differences in intraarticular M-CSF levels among wild-type, *Ccr2*^{-/-}, *Il1rn*^{-/-}, and *Il1rn*^{-/-}*Ccr2*^{-/-} mice (Figure 4C). On the contrary, intraarticular RANKL contents were elevated in *Il1rn*^{-/-} and *Il1rn*^{-/-}*Ccr2*^{-/-} mice, compared with wild-type and *Ccr2*^{-/-} mice, and RANKL levels were higher in *Il1rn*^{-/-}*Ccr2*^{-/-} than *Il1rn*^{-/-} mice (Figure 4C). Similar observations were obtained on intraarticular ADAM 8 contents (Figure 4C). We determined the type(s) of cells expressing RANKL and ADAM 8. Double-color immunofluorescence analysis detected RANKL mainly in Ly-6G-positive neutrophils and CD3-positive T cells, but not F4/80-positive macrophages in synovium (Figure 4D). Likewise, ADAM 8 protein was detected mainly in Ly-6G-positive neutrophils and to a lesser extent, in F4/80-positive macrophages in synovial exudates (Figure 4D). These observations suggest that the absence of *Ccr2* augmented the infiltration of neutrophils, a major source of RANKL and ADAM 8, and that neutrophil-derived RANKL and ADAM 8 in turn can promote osteoclast differentiation from macrophages, which were retained in subchondral bone marrow as well as in synovial tissue.

***Ccr2* deficiency augmented production of neutrophil-tropic chemokines**

In order to delineate the molecular mechanisms underlying enhanced intraarticular neutrophil infiltration, we assessed the intraarticular levels of IL-17A, G-CSF, KC, and

MIP-2, which can potently mobilize neutrophils. IL-17A and G-CSF levels were increased marginally less than 20 pg/mg protein in both *Il1rn*^{-/-} and *Il1rn*^{-/-}*Ccr2*^{-/-} mice (Figure 5A). In contrast, KC and MIP-2 levels were markedly increased in *Il1rn*^{-/-} mice as compared to WT or *Ccr2*^{-/-} mice. Moreover, the increment was further augmented in *Il1rn*^{-/-}*Ccr2*^{-/-} mice. Double-color immunofluorescence analysis revealed that KC and MIP-2 proteins were expressed on Ly-6G-positive neutrophils (Figure 5B, C), as well as on F4/80-positive macrophage but not on CD3 positive T cells (Supplementary Figure 4), suggesting that neutrophils attracted more neutrophils by producing these chemokines in a paracrine manner. These observations indicate that the absence of *Ccr2* gene can amplify intraarticular KC and MIP-2 expression induced by *Il1rn* gene deficiency and that the net result is enhanced neutrophil infiltration in *Il1rn*^{-/-}*Ccr2*^{-/-} mice.

Anti-CXCR2 Ab ameliorated arthritis in *Il1rn*^{-/-}*Ccr2*^{-/-} mice

Finally, to define the involvement of neutrophils in arthritis developed spontaneously in *Il1rn*^{-/-}*Ccr2*^{-/-} mice, we injected antibodies against CXCR2, the predominant receptor for KC and MIP-2, into *Il1rn*^{-/-}*Ccr2*^{-/-} mice between 12 and 16 weeks of age after arthritis became prominent. Anti-mouse CXCR2 antibodies markedly decreased the severity of arthritis (Figure 6A, B) and reduced the infiltration of neutrophils into the joint (Figure 6B). Flow cytometric analysis consistently revealed that the number of neutrophils in the joint was dramatically decreased in anti-CXCR2-treated mice (Figure 6C). Moreover, anti-CXCR2 antibodies markedly reduced osteoclast numbers (Figure 6D). These observations would indicate that CXCR2-mediated neutrophil infiltration crucially contributed to progression of arthritis and pathological osteoclastogenesis in arthritis developed in *Il1rn*^{-/-}*Ccr2*^{-/-} mice.

Discussion

TNF antagonists have been widely used to treat RA patients with a remarkable response rate, compared with conventional therapy. However, not all RA patients benefit sufficiently from TNF antagonist treatment and therefore, an additional therapeutic strategy for RA is needed. TNF antagonists can reduce the biological activities of TNF- α produced mainly by macrophages infiltrating the synovium of RA patients. Because macrophages can produce additional factors involved in progression of arthritis (2), a drug targeting macrophages may be promising for the treatment of RA. CCR2, a receptor for a major macrophage-tropic chemokine, CCL2, may also be an attractive target for the treatment of RA, but the role of CCR2 in arthritis is still controversial. Thus, we examined the effects of *Ccr2* gene ablation on arthritis spontaneously developed in *Il1rn*^{-/-} mice, to delineate the roles of CCR2-mediated signals during the course of the disease. We determined that *Ccr2* gene deletion, to our surprise, markedly augmented arthritis in *Il1rn*^{-/-} mice as evidenced by enhanced bone destruction, together with enhanced intraarticular neutrophil infiltration. Moreover, infiltrating neutrophils expressed two potent osteoclastogenic factors, RANKL and ADAM 8.

Ccr2^{-/-} mice exhibit reduced macrophage infiltration in various types of macrophage-mediated inflammatory responses (32-34). However, in this model, *Ccr2* gene ablation had few effects on macrophage infiltration of the synovium. Quinones and colleagues actually observed enhanced F4/80-positive cell infiltration into the synovium of *Ccr2*^{-/-} mice in collagen-induced arthritis model (14). They further observed that *Ccr2*^{-/-} mice exhibited enhanced intraarticular expression of CCL3, another potent macrophage-tropic chemokine. We also observed that intraarticular expression of CCL5, the chemokine which shares CCR1 and CCR5 with CCL3, was increased in *Il1rn*^{-/-}*Ccr2*^{-/-} compared with *Il1rn*^{-/-} mice (unpublished data). Thus, compensatory CCL5 production may prevent a decrease in macrophage infiltration. Alternatively, increases in infiltrating neutrophils can maintain macrophage infiltration by producing LL37, an α -defensin and heparin-binding protein, which can attract monocytes (35), in a compensatory manner.

Osteoclasts are the main cell type capable of removing calcium from bone and degrading bone matrix and have crucial roles in inflammatory bone erosion. In the first step of inflammatory bone erosion, osteoclast precursor cells, monocytes/macrophages, accumulate near the site of bone erosion (36). *Il1rn*^{-/-} retained a larger number of macrophages in the bone marrow than wild-type mice. Genetic deletion of *Ccr2* resulted in further retention of macrophage in bone marrow. This may mirror the biological activity of the CCL2-CCR2 axis to induce macrophage migration from bone marrow (37). The accumulated macrophages may serve as osteoclast precursor cells. The survival and differentiation of osteoclast progenitor cells, depend on several factors, particularly M-CSF and RANKL (38). Intraarticular RANKL, but not M-CSF, levels were markedly increased in *Il1rn*^{-/-} mice, and the increase was further augmented in *Il1rn*^{-/-}*Ccr2*^{-/-} mice. In addition to RANKL and M-CSF, a member of ADAM family, ADAM 8, can induce osteoclast differentiation, particularly acting at its later phase (39). Moreover, ADAM 8 expression is enhanced in RA pannus adjacent to bone erosion (40), suggesting its crucial contribution to bone erosion in RA. Intraarticular ADAM 8 levels were increased in *Il1rn*^{-/-} and *Il1rn*^{-/-}*Ccr2*^{-/-} mice, similar to RANKL. Thus, it is probable that RANKL and ADAM 8 enhance osteoclastogenesis in *Il1rn*^{-/-} and more so in *Il1rn*^{-/-}*Ccr2*^{-/-} mice, thereby augmenting bone destruction in these mice.

Recent advance in magnetic resonance imaging has revealed that bone edema precedes the onset of bone erosion in RA (30). Histological studies demonstrated that bone edema represents a cellular infiltrate comprising osteoclasts and macrophages within bone, particularly in subchondral bone marrow areas (41). Likewise, osteoclasts and macrophages accumulated in bone marrow in *Il1rn*^{-/-}*Ccr2*^{-/-} mice and to a lesser degree in *Il1rn*^{-/-} mice. Thus, enhanced RANKL and ADAM 8 expression can also induce osteoclast generation in bone marrow, which contained a large number of macrophages, an osteoclast progenitor cell.

Neutrophil infiltration was augmented in various disease models in mice deficient in either *Ccr2* or its ligand, CCL2 (42, 43), as was similarly observed in the present model.

Several independent groups demonstrated that the expression of neutrophil-trophic chemokines, KC/CXCL1 and MIP-2/CXCL2, were enhanced in the absence of either CCR2 or CCL2 (14, 42, 43). We detected the enhanced expression of IL-17A and G-CSF, the cytokines with neutrophil mobilizing activity, in addition to CXCL1 and CXCL2 in joints of *Il1rn*^{-/-} mice. However, only CXCL1 and CXCL2 expression was enhanced to a greater degree in *Il1rn*^{-/-}*Ccr2*^{-/-} than *Il1rn*^{-/-} mice. This may mirror our observation that the intraarticular expression of IL-1 β , a potent inducer of CXCL1 and CXCL2 expression, was enhanced in *Il1rn*^{-/-}*Ccr2*^{-/-} and to a lesser degree in *Il1rn*^{-/-} mice (our unpublished data).

Circulating RANKL levels were not increased in this model (our unpublished data), indicating that RANKL was produced locally in joints as similarly observed in *Streptococcus pyogenes*-induced septic arthritis (44), which is characterized by a massive intraarticular neutrophil infiltration. Thus, infiltrating neutrophils can produce RANKL. This assumption is supported by the previous observations that RANKL is expressed abundantly by RA patient-derived neutrophils and lipopolysaccharide-stimulated neutrophils from normal volunteers (45, 46). Similarly, intraarticularly infiltrating neutrophils were a rich source of RANKL in the present model. In association with the exacerbation of active RA, a large number of neutrophils frequently infiltrate synovial space via pannus (47) and can promote joint damage by releasing reactive oxygen species and lysosomal enzymes. Moreover, ADAM 8 mRNA is detected in human granulocyte and monocytes (48, 49) while ADAM 8 protein is constitutively present on the cell surface and in intracellular granules of human neutrophils and upon activation can be mobilized from the granules to the plasma membrane (49). Likewise, we detected ADAM 8 expression mainly in neutrophils and to a lesser degree in macrophages. The present observations would indicate that the infiltration of neutrophils was amplified in the absence of CCR2 and that infiltrating neutrophils may additionally produce two potent osteoclastogenic molecules, RANKL and ADAM 8, and eventually induce osteoclastogenesis, thereby accelerating bone destruction.

Several lines of evidence indicate that CCL2 can directly act on osteoclasts or

osteoclast progenitor cells to induce osteoclastogenesis (9, 10). Thus, bone destruction in *Il1rn*^{-/-} mice should hypothetically be alleviated by genetic ablation of *Ccr2*, a single and specific receptor for CCL2. However, ablation of *Ccr2* gene markedly increased the infiltration of neutrophils, a cellular source of reactive oxygen species and osteoclastogenic molecules and appears to overcome the direct effect of the CCL2-CCR2 axis on osteoclastogenesis. Moreover, neutrophils are prone to become apoptotic, particularly after being activated and infiltrating, and should be removed by macrophages to prevent tissue injury. This is supported by our report that macrophages can ingest dead neutrophils to promote tissue repair in pneumonia arising from *Pseudomonas aeruginosa* infection in a CCL2-dependent manner (50). Thus, it is probable that macrophages can remove intraarticular infiltrating activated neutrophils, thereby limiting the joint damages in a CCR2-dependent manner. All of these observations may point to a protective role for CCR2-expressing macrophages in an inflammatory joint disease.

Acknowledgment

We express our gratitude to Drs. Joost J. Oppenheim (National Cancer Institute-Frederick, Frederick, MD) for critical review of this manuscript. We thank Drs. William Kuziel for providing us with CCR2-deficient mice.

Auther contributions

All authors were involved in drafting the article or revising it critically for important intellectual content, and all authors approved the final version to be published. Dr. Mukaida had full access to all of the data and the accuracy of the data analysis.

Study conception and design. Mukaida

Acquisition of data. Fujii, Baba, Ishida, Kondo

Analysis and interpretation of data. Fujii, Baba, Yamagishi, Kawano, Mukaida

References

1. McInnes IB, Schett G. Cytokines in the pathogenesis of rheumatoid arthritis. *Nat Rev Immunol.* 2007;7:429-42.
2. Szekanecz Z, Koch AE. Macrophages and their products in rheumatoid arthritis. *Curr Opin Rheumatol.* 2007;19:289-95.
3. Tak PP, Smeets TJ, Daha MR, Kluin PM, Meijers KA, Brand R, et al. Analysis of the synovial cell infiltrate in early rheumatoid synovial tissue in relation to local disease activity. *Arthritis Rheum.* 1997;40:217-25.
4. Haringman JJ, Gerlag DM, Zwinderman AH, Smeets TJ, Kraan MC, Baeten D, et al. Synovial tissue macrophages: a sensitive biomarker for response to treatment in patients with rheumatoid arthritis. *Ann Rheum Dis.* 2005;64:834-8.
5. Mukaida N. Interleukin-8: an expanding universe beyond neutrophil chemotaxis and activation. *Int J Hematol.* 2000;72:391-8.
6. Koch AE. Chemokines and their receptors in rheumatoid arthritis: future targets? *Arthritis Rheum.* 2005;52:710-21.
7. Gong JH, Ratkay LG, Waterfield JD, Clark-Lewis I. An antagonist of monocyte chemoattractant protein 1 (MCP-1) inhibits arthritis in the MRL-lpr mouse model. *J Exp Med.* 1997;186:131-7.
8. Shahrara S, Proudfoot AE, Park CC, Volin MV, Haines GK, Woods JM, et al. Inhibition of monocyte chemoattractant protein-1 ameliorates rat adjuvant-induced arthritis. *J Immunol.* 2008;180:3447-56.
9. Kim MS, Day CJ, Morrison NA. MCP-1 is induced by receptor activator of nuclear factor- κ B ligand, promotes human osteoclast fusion, and rescues granulocyte macrophage colony-stimulating factor suppression of osteoclast formation. *J Biol Chem.* 2005;280:16163-9.
10. Kim MS, Day CJ, Selinger CI, Magno CL, Stephens SR, Morrison NA. MCP-1-induced human osteoclast-like cells are tartrate-resistant acid phosphatase, NFATc1,

and calcitonin receptor-positive but require receptor activator of NF κ B ligand for bone resorption. *J Biol Chem.* 2006;281:1274-85.

11. Haringman JJ, Gerlag DM, Smeets TJ, Baeten D, van den Bosch F, Bresnihan B, et al. A randomized controlled trial with an anti-CCL2 (anti-monocyte chemoattractant protein 1) monoclonal antibody in patients with rheumatoid arthritis. *Arthritis Rheum.* 2006;54:2387-92.

12. Vergunst CE, Gerlag DM, Lopatinskaya L, Klareskog L, Smith MD, van den Bosch F, et al. Modulation of CCR2 in rheumatoid arthritis: a double-blind, randomized, placebo-controlled clinical trial. *Arthritis Rheum.* 2008;58:1931-9.

13. Min SH, Wang Y, Gonsiorek W, Anilkumar G, Kozlowski J, Lundell D, et al. Pharmacological targeting reveals distinct roles for CXCR2/CXCR1 and CCR2 in a mouse model of arthritis. *Biochem Biophys Res Commun.* 391:1080-6.

14. Quinones MP, Ahuja SK, Jimenez F, Schaefer J, Garavito E, Rao A, et al. Experimental arthritis in CC chemokine receptor 2-null mice closely mimics severe human rheumatoid arthritis. *J Clin Invest.* 2004;113:856-66.

15. Bruhl H, Cihak J, Schneider MA, Plachy J, Rupp T, Wenzel I, et al. Dual role of CCR2 during initiation and progression of collagen-induced arthritis: evidence for regulatory activity of CCR2+ T cells. *J Immunol.* 2004;172:890-8.

16. Dinarello CA. Biologic basis for interleukin-1 in disease. *Blood.* 1996;87:2095-147.

17. Dinarello CA. Interleukin-1. *Cytokine Growth Factor Rev.* 1997;8:253-65.

18. Arend WP, Malyak M, Guthridge CJ, Gabay C. Interleukin-1 receptor antagonist: role in biology. *Annu Rev Immunol.* 1998;16:27-55.

19. Guo C, Dower SK, Holowka D, Baird B. Fluorescence resonance energy transfer reveals interleukin (IL)-1-dependent aggregation of IL-1 type I receptors that correlates with receptor activation. *J Biol Chem.* 1995;270:27562-8.

20. Dripps DJ, Brandhuber BJ, Thompson RC, Eisenberg SP. Interleukin-1 (IL-1) receptor antagonist binds to the 80-kDa IL-1 receptor but does not initiate IL-1 signal

transduction. *J Biol Chem.* 1991;266:10331-6.

21. Cohen S, Hurd E, Cush J, Schiff M, Weinblatt ME, Moreland LW, et al. Treatment of rheumatoid arthritis with anakinra, a recombinant human interleukin-1 receptor antagonist, in combination with methotrexate: results of a twenty-four-week, multicenter, randomized, double-blind, placebo-controlled trial. *Arthritis Rheum.* 2002;46:614-24.

22. Tolusso B, Pietrapertosa D, Morelli A, De Santis M, Gremese E, Farina G, et al. IL-1B and IL-1RN gene polymorphisms in rheumatoid arthritis: relationship with protein plasma levels and response to therapy. *Pharmacogenomics.* 2006;7:683-95.

23. Carreira PE, Gonzalez-Crespo MR, Ciruelo E, Pablos JL, Santiago B, Gomez-Camara A, et al. Polymorphism of the interleukin-1 receptor antagonist gene: a factor in susceptibility to rheumatoid arthritis in a Spanish population. *Arthritis Rheum.* 2005;52:3015-9.

24. Horai R, Saijo S, Tanioka H, Nakae S, Sudo K, Okahara A, et al. Development of chronic inflammatory arthropathy resembling rheumatoid arthritis in interleukin 1 receptor antagonist-deficient mice. *J Exp Med.* 2000;191:313-20.

25. Fujikado N, Saijo S, Iwakura Y. Identification of arthritis-related gene clusters by microarray analysis of two independent mouse models for rheumatoid arthritis. *Arthritis Res Ther.* 2006;8:R100.

26. Iizasa H, Yoneyama H, Mukaida N, Katakoka Y, Naito M, Yoshida N, et al. Exacerbation of granuloma formation in IL-1 receptor antagonist-deficient mice with impaired dendritic cell maturation associated with Th2 cytokine production. *J Immunol.* 2005;174:3273-80.

27. Kuziel WA, Morgan SJ, Dawson TC, Griffin S, Smithies O, Ley K, et al. Severe reduction in leukocyte adhesion and monocyte extravasation in mice deficient in CC chemokine receptor 2. *Proc Natl Acad Sci U S A.* 1997;94:12053-8.

28. Delgado M, Abad C, Martinez C, Leceta J, Gomariz RP. Vasoactive intestinal peptide prevents experimental arthritis by downregulating both autoimmune and inflammatory components of the disease. *Nat Med.* 2001;7:563-8.

29. Sonoda Y, Mukaida N, Wang JB, Shimada-Hiratsuka M, Naito M, Kasahara T, et al. Physiologic regulation of postovulatory neutrophil migration into vagina in mice by a C-X-C chemokine(s). *J Immunol.* 1998;160:6159-65.
30. McQueen FM, Benton N, Perry D, Crabbe J, Robinson E, Yeoman S, et al. Bone edema scored on magnetic resonance imaging scans of the dominant carpus at presentation predicts radiographic joint damage of the hands and feet six years later in patients with rheumatoid arthritis. *Arthritis Rheum.* 2003;48:1814-27.
31. Dalbeth N, Smith T, Gray S, Doyle A, Antill P, Lobo M, et al. Cellular characterisation of magnetic resonance imaging bone oedema in rheumatoid arthritis; implications for pathogenesis of erosive disease. *Ann Rheum Dis.* 2009;68:279-82.
32. Boring L, Gosling J, Cleary M, Charo IF. Decreased lesion formation in CCR2^{-/-} mice reveals a role for chemokines in the initiation of atherosclerosis. *Nature.* 1998;394:894-7.
33. Popivanova BK, Kostadinova FI, Furuichi K, Shamekh MM, Kondo T, Wada T, et al. Blockade of a chemokine, CCL2, reduces chronic colitis-associated carcinogenesis in mice. *Cancer Res.* 2009;69:7884-92.
34. Furuichi K, Kaneko S, Wada T. Chemokine/chemokine receptor-mediated inflammation regulates pathologic changes from acute kidney injury to chronic kidney disease. *Clin Exp Nephrol.* 2009;13:9-14.
35. Soehnlein O, Lindbom L, Weber C. Mechanisms underlying neutrophil-mediated monocyte recruitment. *Blood.* 2009;114:4613-23.
36. Schett G. Osteoimmunology in rheumatic diseases. *Arthritis Res Ther.* 2009;11:210.
37. Serbina NV, Pamer EG. Monocyte emigration from bone marrow during bacterial infection requires signals mediated by chemokine receptor CCR2. *Nat Immunol.* 2006;7:311-7.
38. Asagiri M, Takayanagi H. The molecular understanding of osteoclast differentiation. *Bone.* 2007;40:251-64.

39. Choi SJ, Han JH, Roodman GD. ADAM8: a novel osteoclast stimulating factor. *J Bone Miner Res.* 2001;16:814-22.
40. Ainola M, Li TF, Mandelin J, Hukkanen M, Choi SJ, Salo J, et al. Involvement of a disintegrin and a metalloproteinase 8 (ADAM8) in osteoclastogenesis and pathological bone destruction. *Ann Rheum Dis.* 2009;68:427-34.
41. McQueen FM, Ostendorf B. What is MRI bone oedema in rheumatoid arthritis and why does it matter? *Arthritis Res Ther.* 2006;8:222.
42. Montgomery RR, Booth CJ, Wang X, Blaho VA, Malawista SE, Brown CR. Recruitment of macrophages and polymorphonuclear leukocytes in Lyme carditis. *Infect Immun.* 2007;75:613-20.
43. Sawanobori Y, Ueha S, Kurachi M, Shimaoka T, Talmadge JE, Abe J, et al. Chemokine-mediated rapid turnover of myeloid-derived suppressor cells in tumor-bearing mice. *Blood.* 2008;111:5457-66.
44. Sakurai A, Okahashi N, Nakagawa I, Kawabata S, Amano A, Ooshima T, et al. Streptococcus pyogenes infection induces septic arthritis with increased production of the receptor activator of the NF-kappaB ligand. *Infect Immun.* 2003;71:6019-26.
45. Poubelle PE, Chakravarti A, Fernandes MJ, Doiron K, Marceau AA. Differential expression of RANK, RANK-L, and osteoprotegerin by synovial fluid neutrophils from patients with rheumatoid arthritis and by healthy human blood neutrophils. *Arthritis Res Ther.* 2007;9:R25.
46. Chakravarti A, Raquil MA, Tessier P, Poubelle PE. Surface RANKL of Toll-like receptor 4-stimulated human neutrophils activates osteoclastic bone resorption. *Blood.* 2009;114:1633-44.
47. Pillinger MH, Abramson SB. The neutrophil in rheumatoid arthritis. *Rheum Dis Clin North Am.* 1995;21:691-714.
48. Yoshiyama K, Higuchi Y, Kataoka M, Matsuura K, Yamamoto S. CD156 (human ADAM8): expression, primary amino acid sequence, and gene location. *Genomics.* 1997;41:56-62.

49. Gomez-Gavero M, Dominguez-Luis M, Canchado J, Calafat J, Janssen H, Lara-Pezzi E, et al. Expression and regulation of the metalloproteinase ADAM-8 during human neutrophil pathophysiological activation and its catalytic activity on L-selectin shedding. *J Immunol.* 2007;178:8053-63.
50. Amano H, Morimoto K, Senba M, Wang H, Ishida Y, Kumatori A, et al. Essential contribution of monocyte chemoattractant protein-1/C-C chemokine ligand-2 to resolution and repair processes in acute bacterial pneumonia. *J Immunol.* 2004;172:398-409.

Legends to Figures

Figure 1. Enhanced arthritis in *Il1rn*^{-/-} mice by *Ccr2* gene ablation

(A) Body weights and arthritis scores were determined weekly. Mean and SD were calculated and are shown here (*Il1rn*^{-/-} mice, n = 40; *Il1rn*^{-/-}*Ccr2*^{-/-} mice, n=50). *, $p < 0.05$; #, $p < 0.01$. (B) Ankle joints were removed at the indicated time intervals, fixed, and stained with hematoxylin and eosin. Representative results from 5 animals for each genotype and scoring of cartilage damage, bone erosion, and cell infiltration are shown here. Bars, 100 μm . Mean and SD were calculated and are shown here (n=5 for each group). *, $p < 0.05$. (C) Total bone mineral density (BMD) of fore limbs was measured with computed tomography on 20-week old mice. Mean and SD were calculated and are shown here (n = 16 to 55 for each genotypes). *, $p < 0.05$; ***, $p < 0.001$. (D) Serum levels of COMP were determined by ELISA at 20 week of age. Mean was calculated and are shown here (n= 6 to 10 animals). *, $p < 0.05$.

Figure 2. Enhanced intraarticular neutrophil accumulation in *Il1rn*^{-/-}*Ccr2*^{-/-} mice.

(A) The numbers of CD3-, F4/80-, or Ly-6G positive cells in ankle joints were enumerated as described in Materials and Methods. Mean and SD were calculated and are shown here (n = 6 animals). *, $p < 0.05$. (B) and (C) Single cell suspensions were obtained from the joint cavity of 10- or 20-week-old *Il1rn*^{-/-} or *Il1rn*^{-/-}*Ccr2*^{-/-} mice and were stained with various combinations of antibodies and analyzed with FACS as described in Materials and Methods. Ly-6G and Ly-6C profiles in CD11b⁺ cells from joints were determined and representative results from 5 independent animals are shown in B. Absolute cell number in each fraction was calculated. Mean and SD were calculated (n=5) and are shown in c. *, $p < 0.05$.

Figure 3. Increased intraarticular osteoclasts in *Il1rn*^{-/-}*Ccr2*^{-/-} mice

(A) The numbers of TRAP-positive osteoclasts were counted as described in Material and

Methods. Mean and SD were calculated and are shown here (n=5). (B) Serum TRAP5b concentration was determined on 20-week old mice by ELISA. Mean and SD were calculated and are shown here (n = 6 to 15 animals). *, $p < 0.05$ vs. *Il1rn*^{-/-} mice.

Figure 4. Increased osteoclast precursors and osteoclastogenic factors in *Il1rn*^{-/-}*Ccr2*^{-/-} mice

(A) The numbers of TRAP-positive osteoclasts in subchondral bone marrow regions were enumerated as described in Material and Methods. Mean and SD were calculated and are shown here (n=5). *, $p < 0.05$; ***, $p < 0.01$; n.s., not significant. (B) Bone marrow cells were obtained from 8- or 20-week old mice and were stained with a combination of PE-labeled anti-CD11b, APC-labeled anti-Ly-6G, and FITC-labeled anti-Ly-6C antibodies. The proportion of CD11b⁺Ly-6G^{int}Ly-6C⁺ monocytes was enumerated based on the results from FACS analysis. Mean and SD were calculated and are shown here (n = 5 animals). *, $p < 0.05$; #, $p < 0.01$. (C) M-CSF, RANKL, and ADAM 8 contents were determined on joints obtained from 20-week-old animals by using specific ELISA as described in Material and Methods. Mean and SEM were calculated and are shown here (n = 15 to 20 animals). *, $p < 0.05$; #, $p < 0.01$. (D) Ankle joints were removed from 20-week-old *Il1rn*^{-/-}*Ccr2*^{-/-} mice, and were subjected to staining with the combination of anti-RANKL and anti-Ly-6G, anti-RANKL and anti-CD3, or anti-RANKL and anti-F4/80 antibodies as described in Material and Methods. Cytospin sections were prepared from joint exudates from 20-week-old *Il1rn*^{-/-}*Ccr2*^{-/-} mice and stained with the combination of anti-ADAM 8 and anti-Ly-6G, anti-ADAM 8 and anti-CD3, or anti-ADAM 8 and anti-F4/80 antibodies. Representative results from 3 independent animals are shown here. Bars, 20 μ m.

Figure 5. Augmented chemokine production in *Il1rn*^{-/-}*Ccr2*^{-/-} mice.

(A) IL-17A, G-CSF, KC, and MIP-2 contents were determined on joints obtained from 20-week-old animals as described in Material and Methods. Mean and SEM were calculated and are shown here (n = 8 to 16 animals). *, $p < 0.05$; #, $p < 0.01$. (B)(C) Ankle

joints were removed from 20-week-old *Il1rn^{-/-}Ccr2^{-/-}* mice, and were subjected to staining with the combinations of anti-KC and anti-Ly6G (B) or anti-MIP-2 and anti-Ly-6G antibodies (C) as described in Material and Methods. Representative results from 3 independent animals are shown here. Bars, 20 μ m.

Figure 6. Anti-CXCR2 Ab ameliorated arthritis development in *Il1rn^{-/-}Ccr2^{-/-}* mice

(A) *Il1rn^{-/-}Ccr2^{-/-}* mice received intraperitoneally either anti-mouse CXCR2 or control antibodies, twice a week from 12 weeks of age until 16 weeks of age. Arthritis scores were determined weekly. Mean and SEM were calculated and are shown here (n=7). (B) The appearance and HE staining of the hind feet of the IgG treated and anti-mouse CXCR2 Ab-treated mice on 16 weeks of age are shown. Representative results from 7 animals are shown here. Bars, 50 μ m. (C) Single cell suspensions were obtained from the joint cavity of 16-week-old mice and were stained with the combination of CD11b and Ly-6G antibodies and analyzed with FACS as described in Material and Methods. Absolute cell number in CD11b⁺Ly-6G⁺ fraction was calculated. Mean and SEM were calculated (n=7). (D) The numbers of TRAP-positive osteoclasts were counted as described in Material and Methods. Mean and SD were calculated and are shown here (n=5). *, $p < 0.05$. #, $p < 0.01$.

Supplementary Figure 1. Immunohistochemical detection of CD3-, F4/80-, or Ly-6G-positive cells in ankle joints.

Ankle joints were removed at the indicated time intervals from *Il1rn^{-/-}* mice and *Il1rn^{-/-}Ccr2^{-/-}* mice and immunostained with anti-CD3, anti-F4/80, or anti-Ly-6G antibody as described in Materials and Methods. Boxed areas are shown at higher magnification in the right panels. Representative results from 6 independent animals are shown here. Bars, 100 μ m.

Supplementary Figure 2. TRAP-positive cells in joints and subchondral bone marrow.

(A) Ankle joints were removed at the indicated time intervals, and were stained for TRAP.

Representative results from 5 individual mice are shown here. Original magnification, x 100. (B) Subchondral bone marrow beneath joint cavities was obtained from 20-week old mice and was subjected to TRAP staining. Representative results from 3 independent animals are shown here. Bars, 100 μm .

Supplementary Figure 3. Increased monocytes in the bone marrow of *Il1rn*^{-/-}*Ccr2*^{-/-} mice

Bone marrow cells were obtained from 20-week old mice and were stained with a combination of PE-labeled anti-CD11b, APC-labeled anti-Ly-6G, and FITC-labeled anti-Ly-6C antibodies. Representative results from 5 mice are shown here.

Supplementary Figure 4. Immunohistochemical detection of KC and MIP-2 producing cells in ankle joints

Ankle joints were removed from 20-week-old *Il1rn*^{-/-}*Ccr2*^{-/-} mice, and were subjected to staining with the combinations of anti-KC and anti-CD3, anti-KC and anti-F4/80, anti-MIP-2 and anti-CD3, or anti-MIP-2 and anti-F4/80 antibodies as described in Material and Methods. Representative results from 3 independent animals are shown here. Bars, 20 μm .

Figure 1 Fujii et al

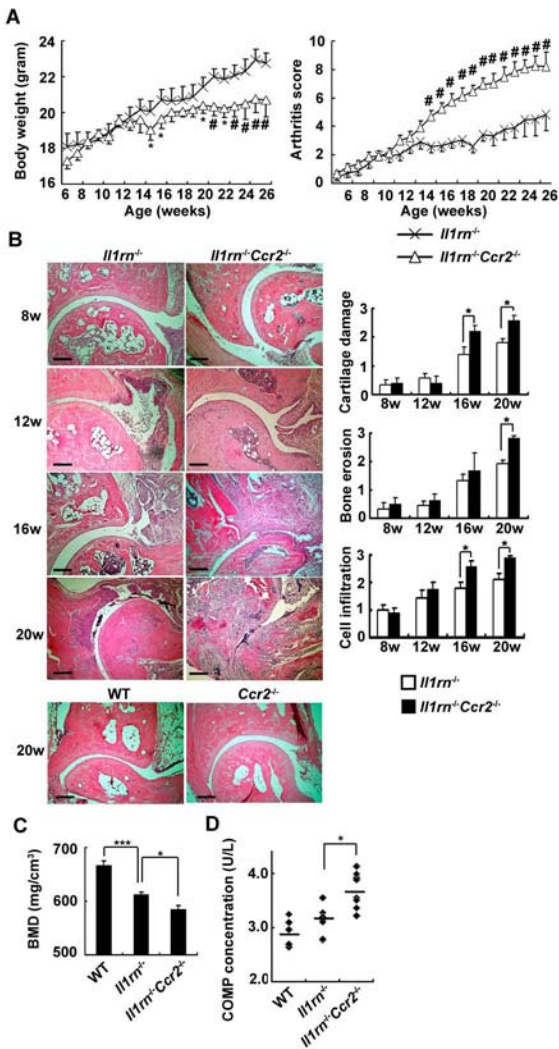
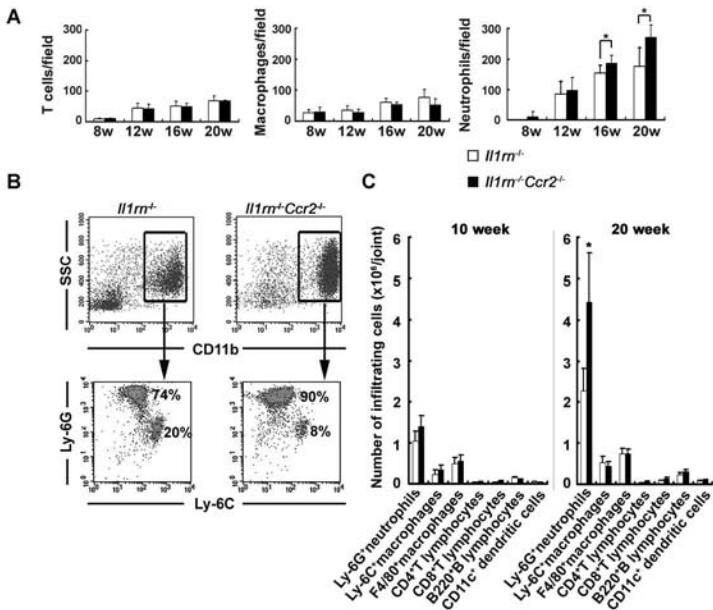


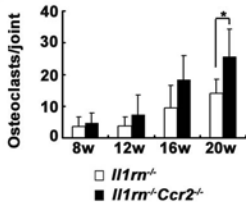
Figure 2 Fujii et al



Top ↑

Figure 3 Fujii et al

A



B

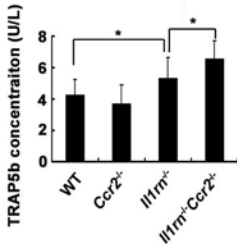
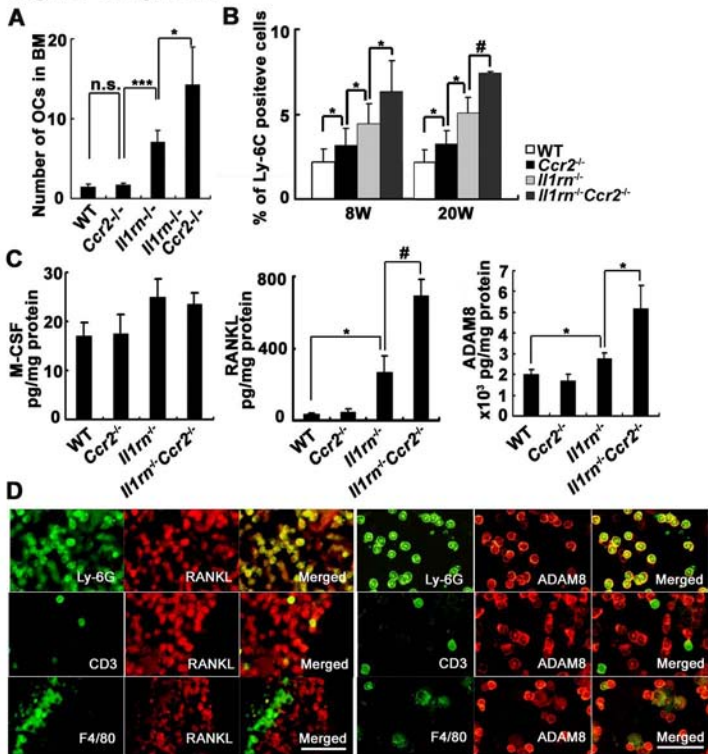


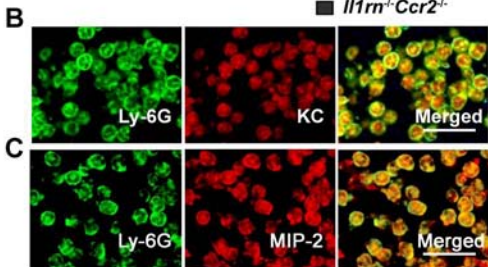
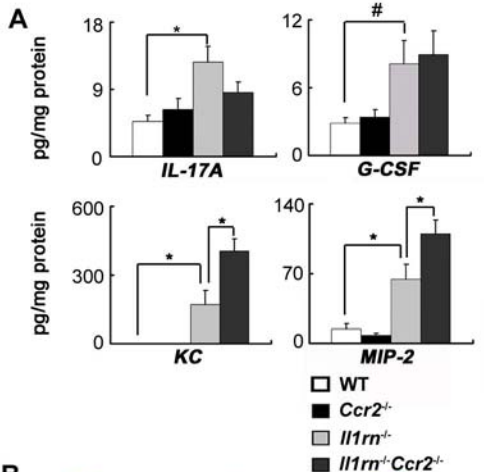
Figure 4 Fujii et al

Top ↑



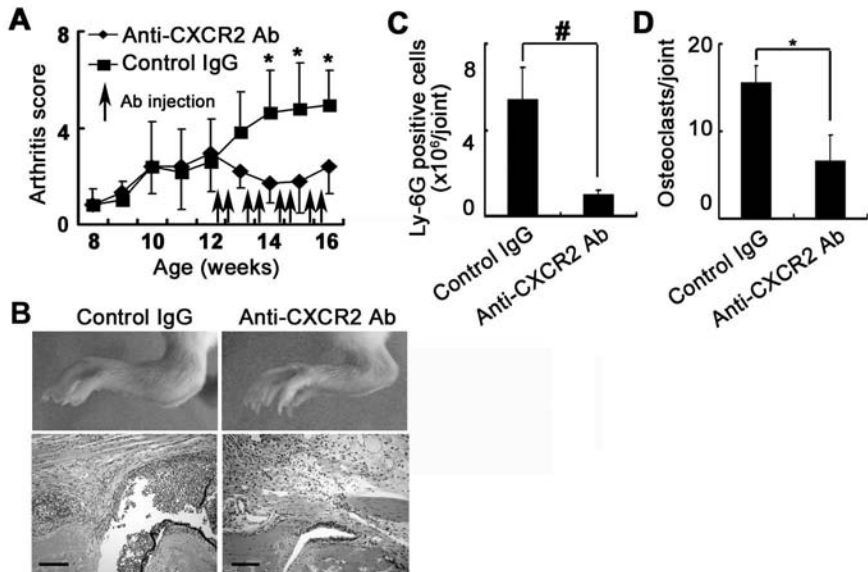
Top ↑

Figure 5 Fujii et al



Top ↑

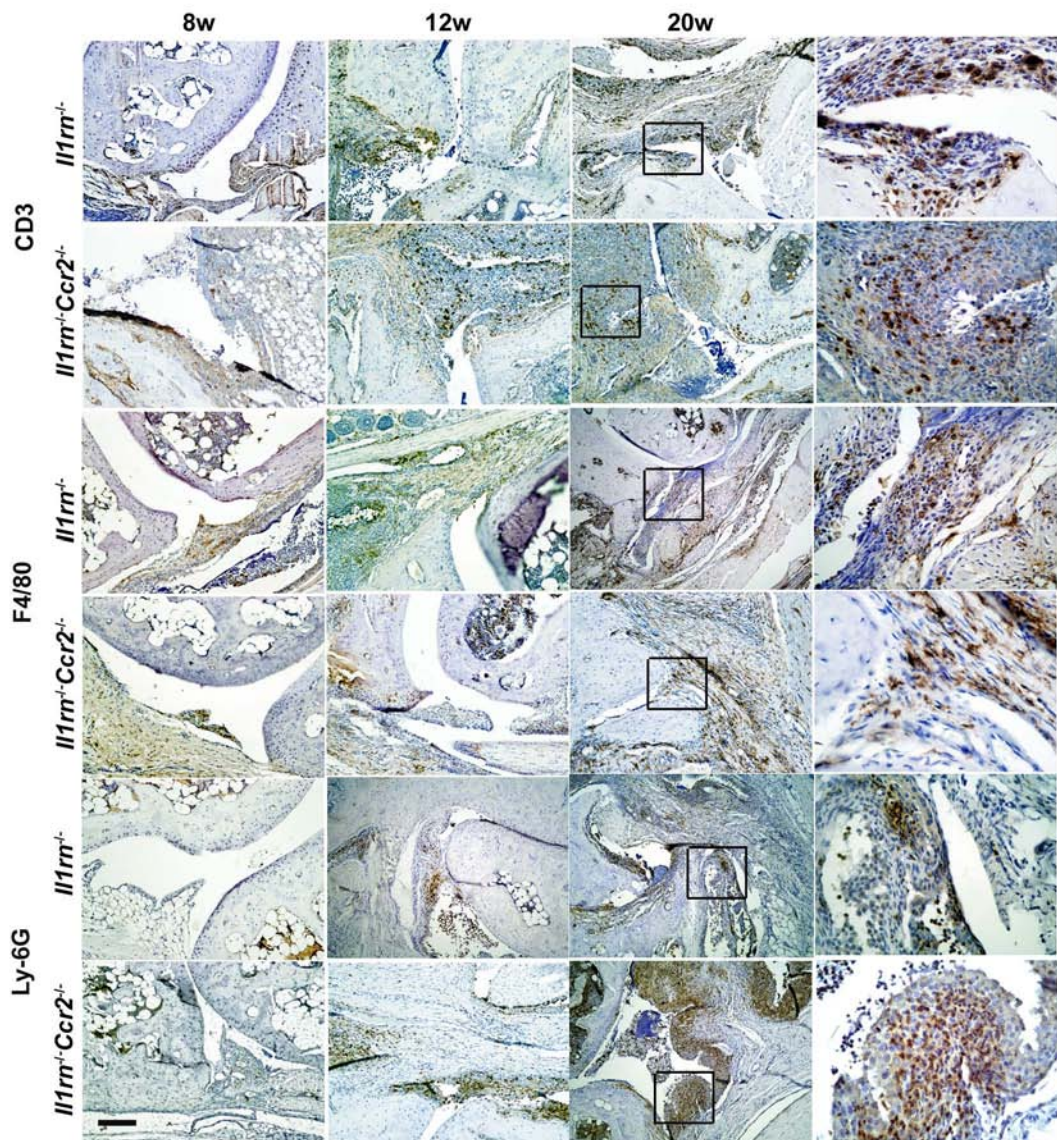
Figure 6 Fujii et al



Top ↑

Supplementary Figure 1 Fujii et al

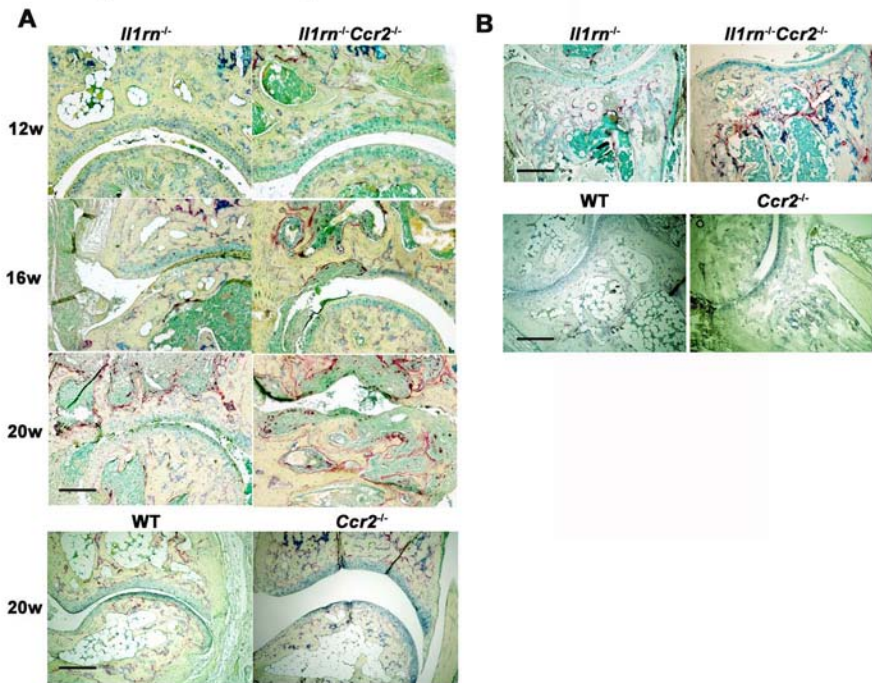
Immunohistochemical detection of CD3-, F4/80-, or Ly-6G-positive cells in ankle joints



Top ↑

Supplementary Figure 2 Fujii et al

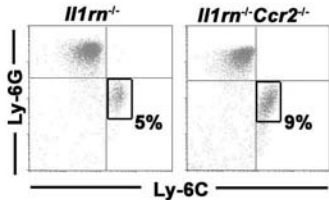
TRAP-positive cells in joints and subchondral bone marrow



Top ↑

Supplementary Figure 3 Fujii et al

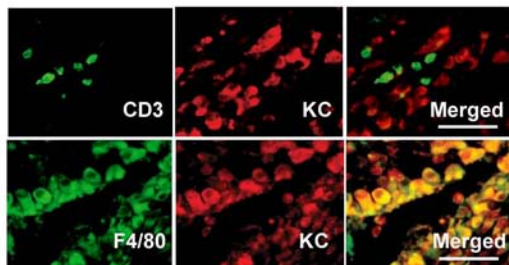
Increased monocytes in the bone marrow of *Il1rn^{-/-}Ccr2^{-/-}* mice



Supplementary Figure 4 Fujii et al

Immunohistochemical detection of KC and MIP-2 producing cells in ankle joints

A



B

